NO stock 605 copies

IDO-1601-2

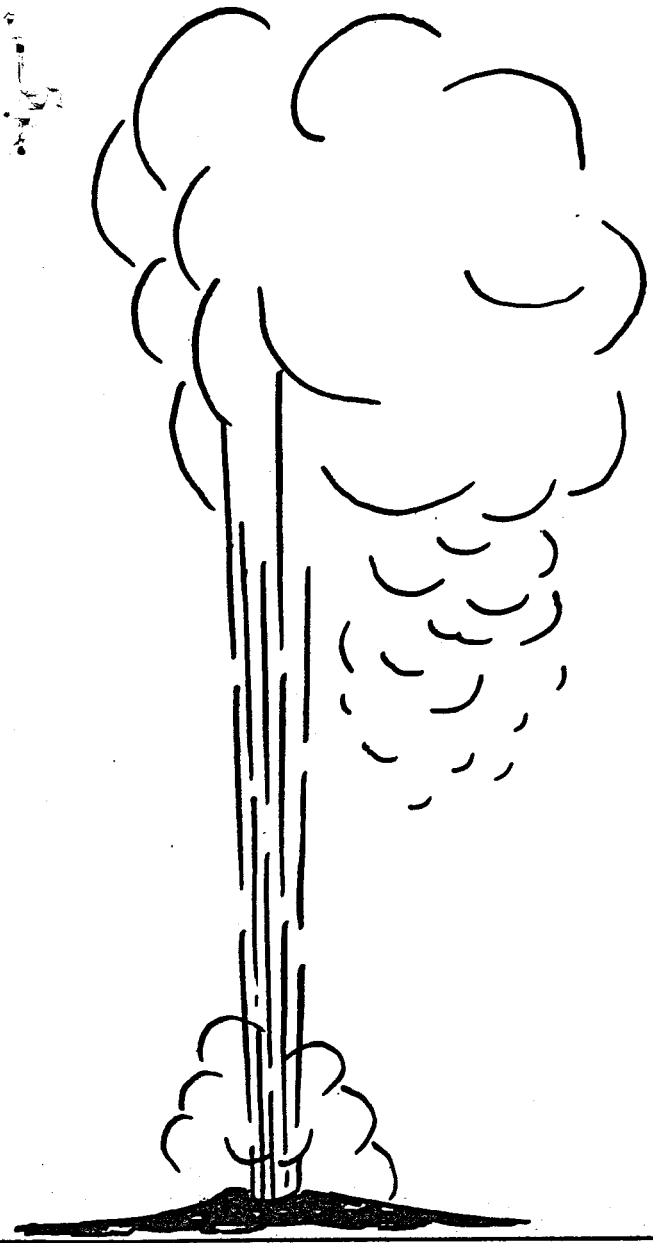

LOW-ALTITUDE AEROMAGNETIC SURVEY OF A PORTION OF THE COSO HOT SPRINGS KGRA INYO COUNTY, CALIFORNIA

By
Richard C. Fox

May 1978
Date Published

Work Performed Under Contract No. EY-76-S-07-1601

Earth Science Laboratory
University of Utah Research Institute
Salt Lake City, Utah

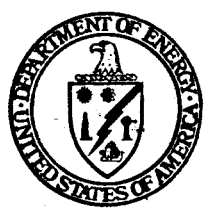

U. S. DEPARTMENT OF ENERGY
Geothermal Energy

MASTER

DISCLAIMER

NOTICE

Available from the National Technical Information Service, U. S. Department of Commerce, Springfield, Virginia 22161.

Price: Paper Copy $4.50
Microfiche $3.00

Printed in the United States of America
USDOE Technical Information Center, Oak Ridge, Tennessee

IDO-1601-2
Distribution Category UC-66a

LOW-ALTITUDE AEROMAGNETIC SURVEY OF A PORTION OF THE COSO HOT SPRINGS KGRA, INYO COUNTY, CALIFORNIA

Richard C. Fox

EARTH SCIENCE LABORATORY
UNIVERSITY OF UTAH RESEARCH INSTITUTE
391-A Chipeta Way
Salt Lake City, Utah 84108

Date Published - May 1978

Prepared for the
DEPARTMENT OF ENERGY
DIVISION OF GEOTHERMAL ENERGY
UNDER CONTRACT EY-76-S-07-1601

NOTICE

Reference to a company or product name does not imply approval or recommendation of the product by the University of Utah Research Institute or the U.S. Department of Energy to the exclusion of others that may be suitable.

TABLE OF CONTENTS

LIST OF ILLUSTRATIONS

ABSTRACT

A detailed low-altitude aeromagnetic survey of 576 line-mi (927 line-km) was completed over a portion of the Coso Hot Springs KGRA in September 1977. The survey has defined a pronounced magnetic low that could help delineate the geothermal system. The magnetic low has an areal extent of approximately 10 sq mi (26 sq km). Direct and indirect evidence indicates that this anomaly is due, in part, to magnetite destruction by hydrothermal solutions associated with the geothermal system. The anomaly generally coincides with two other geophysical anomalies which are directly associated with the system: 1) a bedrock electrical resistivity low, and 2) an area of relatively high near-surface temperatures. The highest measured heat flow, 18 HFU, also occurs within its boundary.

The magnetic low occurs at the intersection of two major structural zones which coincide with a complementary set of strike-slip fault zones determined from seismic activity. The intersection of these two zones of active tectonism probably served as the locus for emplacement of a pluton at depth, above which are observed the coincidental geophysical anomalies and surface manifestations related to the geothermal system.

INTRODUCTION

On behalf of the U.S. Department of Energy, Division of Geothermal Energy, geological and geophysical studies were conducted for a portion of the Coso Hot Springs KGRA (Fig. 1) by the Earth Science Laboratory, University of Utah Research Institute. These studies served two purposes: 1) evaluation and interpretation of results from the drilling and logging of CGEH-1 (Galbraith, 1978), and 2) determination of possible sites for future drill tests. Investigations for the latter were carried out during September and October, 1977 and included geologic and alteration mapping (Hulen, 1978), a detailed electrical resistivity survey (Fox, 1978) and a low-altitude aeromagnetic survey, the results of which are the subject of this report.

A regional aeromagnetic survey of the Coso area was completed in 1975 by the U.S. Geological Survey (Open-file report 76-698) which covered an area 32 mi E-W by 30 mi N-S (51 by 48 km) centered approximately on Coso Hot Springs. The survey altitude was 7000 feet (2135 m) above sea level, approximately 2500 feet (762 m) above the mean terrain elevation of the present survey area, and the flight line spacing was one mile (1.6 km). These survey characteristics precluded the recording of local, small scale changes in magnetization.

The present survey was flown to generate a detailed magnetic map that could show local variations in rock magnetization and magnetic features related to structures that would help delineate the geothermal system.

GEOLOGY

The Coso Range, in which the Coso KGRA is located, occurs in the western Basin and Range province. It was formed primarily by dip-slip movement along


CALIFORNIA
0 20 40 60 80
MILES
N
LOCATION MAP
COSO HOT SPRINGS
KGRA
OREGON
DEL NORTE
Crescent City
Yreka
SISKIYOU
MODOC
Alturas
HUMBOLDT
Eureka
TRINITY
Weaverville
SHASTA
Redding
LASSEN
Susanville
Red Bluff
TEHAMA
PLUMAS
Quincy
MENDOCINO
GLENN
Willows
BUTTE
Oroville
SIERRA
Downieville
COLUSA
NEVADA
Nevada City
Ukiah
Lake-port
Colusa
Yuba City
YUBA
Marysville
PLACER
LAKE
Auburn
YOLO
SUTTER
EL DORADO
Placerville
SONOMA
NAPA
Wood-land
Sacramento
Markleeville
Santa Rosa
Napa
Fair-field
SACRA-MENTO
AMADOR
Jackson
ALPINE
CALAVERAS
Bridgeport
MARIN
SOLANO
SAN JOAQUIN
San Andreas
TUOLUMNE
San Rafael
Martinez
CONTRA COSTA
Stockton
Sonora
San Francisco
SAN FRANCISCO
Oakland
ALAMEDA
Modesto
MARIPOSA
Mariposa
MONO
Redwood City
SAN MATEO
San Jose
STANISLAUS
Merced
MADERA
SANTA CLARA
SANTA CRUZ
Santa Cruz
MERCED
Madera
FRESNO
Hollister
Salinas
SAN BENITO
Fresno
Independence
Hanford
Visalia
INYO
MONTEREY
KINGS
TULARE
SAN LUIS OBISPO
Bakersfield
San Luis Obispo
KERN
SAN BERNADINO
SANTA BARBARA
VENTURA
LOS ANGELES
Santa Barbara
Ventura
San Bernardino
Los Angeles
Riverside
Santa Ana
RIVERSIDE
ORANGE
ARIZ
SAN DIEGO
IMPERIAL
El Centro
San Diego
MEXICO

FIGURE 1

northerly-trending, high-angle normal faults. Within the survey area, the Basin and Range structure is disrupted by west-northwest, northwest and north-trending high-angle faults. Plate I covers the survey area and a corresponding portion of the Coso Range as mapped by Duffield and Bacon (1977). This map shows the surface geology as a Late Cenozoic basaltic to rhyolitic volcanic sequence resting on a Mesozoic (?) basement complex.

The volcanic sequence includes several prominent rhyolitic domes and a lesser number of basaltic domes. Although the basement complex is not subdivided on this map, Duffield and Bacon (1977, sheet 2) indicate that it consists principally of granitic intrusive rock and ranges in composition from granite through quartz-diorite to diorite or gabbro. Hulen (1978) in an accompanying report states that the granitic intrusives, Jurassic-Late Cretaceous in age, are probably satellites of the southern Sierra Nevada Batholith.

AEROMAGNETIC SURVEY

The total-field aeromagnetic survey was conducted by Aerial Surveys of Salt Lake City, Utah. The survey flown in September, 1977 covers an area extending 12 mi N-S by 12 mi (19 km sq) E-W, centered on Devil's Kitchen. The flight altitude was 750 feet (229 m) above mean terrain with a one-quarter mile (403 m) line spacing. A total of 576 line-mi (927 line-km) was surveyed. Data were recorded in analog format and digitally on magnetic tape. The terrain clearance along the flight line was maintained by digital readout from a radar altimeter during the survey and was continuously recorded in analog form on a strip chart recorder. A continuously recording ground magnetic

station recorded diurnal changes in the magnetic field and monitored magnetic storm activity. Topographic base maps for the surveyed area include the USGS 15 minute topographic series quadrangles of Haiwee Reservoir, Coso Peak, Little Lake and Mountain Springs Canyon.

The survey results were compiled manually. A flight line map was made by matching images on 35 mm strip film of the flight lines to images on aerial photographs (scale 1:18,000) of the surveyed area taken at the start of the survey. Intermediate points along each flight line were located by linear interpolation between the recovered points. The flight lines located on the aerial photo base were rectified to an accurate topographic base by transforming points from the photo base to corresponding points on a 1:18,000 scale topographic map. Magnetic values for fiducial numbers corresponding with the recovered points and maximum and minimum magnetic values observed between recovered points were taken from the analog records and posted along the flight lines. The final map was compiled at a scale of 1:24,000 with a 25 gamma contour interval. A base level value of 50,000 gammas was subtracted from the observed total field values.

INTERPRETATION

Magnetic Anomalies

The sources of several magnetic anomalies were identified by correlating the magnetic anomalies, Plate II, with the topography and geology, Plate I. These anomalies are identified by reference points (RP) on Plate III. The source outlines shown on this plate are only approximate outlines of the actual magnetic sources and are shown mainly for the purpose of locating the

source areas. Table I shows the probable source rock type, and probable causes of the anomalies. Except for RP-17, all of the identified anomalies have sources that are attributable to the outcropping rock in their source areas.

TABLE I

Interpretation of Magnetic Anomaly Sources

Reference Point	Probable Rock Type	Probable Cause
RP - 1, 2, 3, 17	Diorite or Gabbro	SC*
RP - 4, 6, 7, 8, 9, 10, 11, 13, 14, 15, 18, 19, 20, 25, 29, 30, 31	Rhyolite	SC+TE*+RM*
RP - 5, 23, 26, 27, 28 40	Basalt	SC+TE+RM
RP - 12	Dacite	SC+TE+RM
RP - 16, 22, 34, 35	Basalt	SC+RM
RP - 21	Granite(?)	SC+TE
RP - 24	Andesite	SC+TE+RM
RP - 32, 33, 36, 37, 38, 39	Quartz-diorite(?)	TE

*SC = Susceptibility Contrast
*TE = Terrain Effect
*RM = Remanent Magnetization

Many of these anomalies show a strong correlation with topography, e.g., the rhyolite domes. Topographic-effect magnetic anomalies are caused by magnetic terrain features. Variations in terrain clearance between the airborne magnetometer and the topographic surface can significantly contribute to the observed anomalies, especially in a low altitude survey like this. Both magnetic highs and lows can be generated by topographic features as shown by Figure 2.

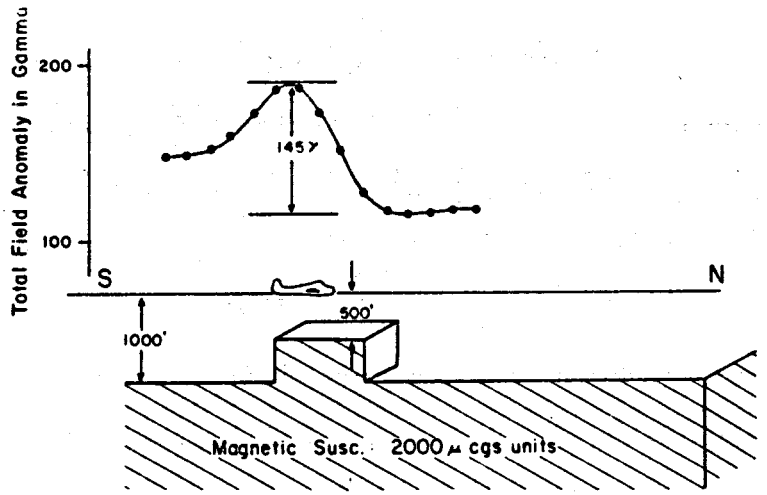

Topo Feature

width	length	height
1000'	1000'	500'

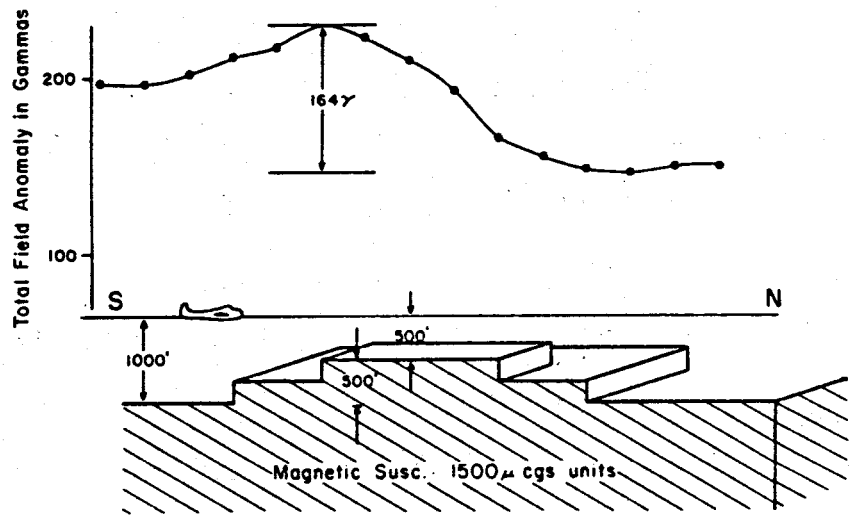

Topo Feature

width	length	height
4000'	4000'	250'
2000'	2000'	250'

Total Relief 500'

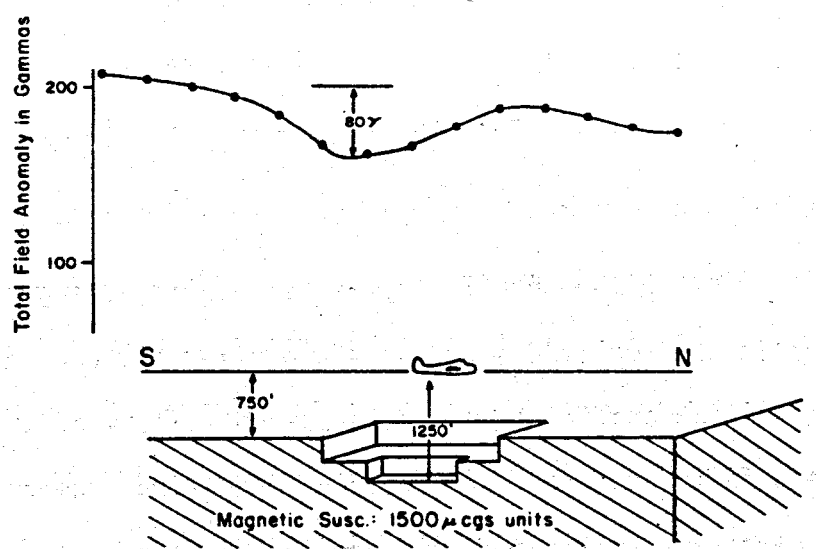

Topo Feature

width	length	depth
2000'	2000'	250'
1000'	1000'	250'

Total Relief 500'

FIGURE 2

TOPOGRAPHIC EFFECT MAGNETIC ANOMALIES

Earth's Magnetic Field Strength: 50,000 gammas
Declination = 16°E; Inclination = 60°

Preliminary attempts to determine the magnetization and source geometry for the rhyolite domes indicated some degree of remanent magnetization contributed to their observed anomalies. Various domes were individually modelled using vertical-sided, right-regular prisms with 10,000 ft (3050 m) of depth extent. The area of the models, in plan view, approximated the outcrop area of the individual domes as shown on Plate I. The apparent magnetic susceptibilities assigned to these models to match the observed anomalies are in the range 1000-2000 micro-cgs units. To make the geometry of these simple models conform more closely to a reasonable geometry for the root systems of the domes, e.g. an inverted cone or funnel, would cause an attendant volume decrease which would have to be offset by an increase in apparent magnetic susceptibility. Apparent susceptibilities larger than 2000 micro-cgs are unusual for rhyolites in general and could be explained by a remanent magnetization component. The magnetic susceptibility of a rock, k, is the ratio of the intensity of its induced magnetic anomaly, I, to the intensity of the inducing magnetic field, H; that is $k = \frac{I}{H}$. If a rock is permanently magnetized in a direction that adds to the magnetic anomaly due only to induction by the earth's magnetic field, it will have an interpreted or apparent susceptibility that is higher than the true susceptibility expected for the given rock type.

A common feature of most of the rhyolite domes is a positive magnetic expression. Variations in the amplitudes of their anomalies are due to several factors such as variations in: 1) magnetic susceptibility of the domes or between the domes and their host rock, 2) remanent magnetization, 3) terrain clearance, or 4) flight line location. None of these factors readily

explain the lack of magnetic expression of the dome at RP-15a (Plate III). Either this dome has no appreciable root system (volume of magnetic material) or, if it does, the magnetite within its root structure has been altered by hydrothermal solutions to non-magnetic hematite or pyrite. If the latter explanation is the actual case, the age determined for this dome of less than 100,000 years (Lanphere and Dalrymple, 1975) suggests that the magnetite alteration could be caused by hydrothermal fluids associated with the present geothermal system.

Basement Magnetization

Broad west-northwest trending zones of contrasting magnetic intensity have been delineated on Plate III that define the gross magnetic characteristics of the area. The intensity levels assigned to each zone are taken from the contoured magnetic values shown on Plate II. These are residual total magnetic field values after a base level of 50,000 gammas was subtracted from the observed values. The two zones of low magnetic intensity, generally less than 1000 gammas, are interpreted to be caused by granitic basement rock. The zones of intermediate magnetic intensity, 1000 to 1200 gammas, are attributed to quartz-diorite and the high magnetic intensity zones, greater than 1200 gammas, to the diorite or gabbro end of the basement composition range. The margins of these zones are gradational between intermediate and high intensity zones but sharp between low and intermediate and between low and high zones. The sharp gradients are, in part, coincidental with west-northwest, trending mapped faults (Plate I) and thus may represent structural boundaries between adjacent zones. The sharp boundary between the southernmost low magnetic intensity zone and the adjacent

intermediate zone may be the northern edge of the west-northwest trending Wilson Canyon fault system which projects through this area (Furgerson, 1975, pg. 2). The sharp boundary between the zone of low magnetic intensity associated with the Haiwee trend and the zone of high magnetic intensity to the south may reflect the southern edge of the Haiwee fault system.

A magnetic profile that crosses the three levels of magnetic intensity (see Plate III for location) was analyzed to determine the range of apparent magnetic susceptibilities that are associated with these levels. Figure 3 shows the observed and computed magnetic gradient and the model used to make the analysis. As constructed, the model takes into account the variation in terrain clearance along the profile as observed on the terrain clearance analog record for this profile. Each prism of the model extends 10,000 feet (3500 m) to the east and to the west of the profile to approximate the general east-west linear trend in terrain elevation (Plate I) and to produce the observed east-west linear trend in magnetic intensity (Plate II). The prisms extend to 10,000 feet below the line of observation. This depth extent was chosen to insure that the computed magnetic gradient would be only a function of the topographic relief and the horizontal change in magnetic susceptibility and would not be influenced by the depth extent of the prisms. Figure 3 shows that an increase in magnetic susceptibility of 3000 micro cgs units across the zones from low to high magnetic intensity is required to generate the observed gradient.

Magnetic susceptibilities were measured on ten foot (3 m) samples of drill cuttings from 430 intervals of drill hole CGEH-1. The samples were

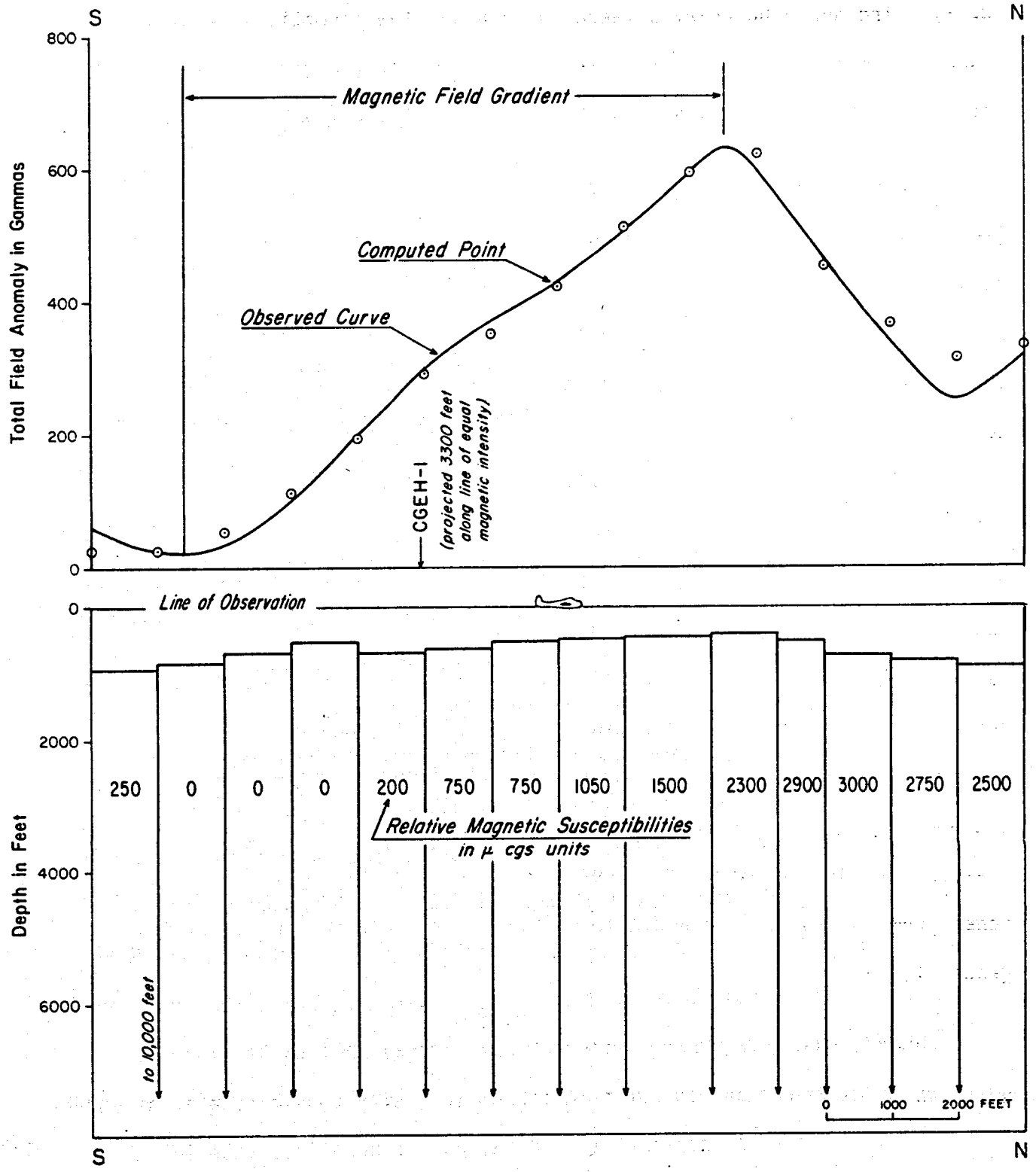

FIGURE 3

ANALYSIS OF MAGNETIC FIELD GRADIENT

(see Plate 3 for location of profile)

placed into four general categories according to composition (Galbraith, 1978), that are consistent with those used by Hulen (1978) to group the surface rocks he observed within this area. These categories are: 1) an older, pre-Late Cretaceous intermediate-to-mafic metamorphic sequence, 2) post-metamorphic quartz-latite porphyry and felsite, 3) Late Cretaceous (?) granite and allied intrusives (leucogranite and alaskite) and 4) Late Cenozoic volcanics (rhyolite). Based upon thin-section analysis, these rock types encountered in CGEH-1 appear only slightly altered (Galbraith, 1978). The majority of samples fall in either the metamorphic or granite and allied intrusive categories. The average magnetic susceptibility value for 154 samples in the metamorphic category is 1118 micro cgs units with a standard deviation of 849 micro cgs; that for 143 samples in the granite and allied intrusive category is 547 micro cgs units with a deviation of 566 micro cgs. Because of the weak susceptibility contrast (about 500 micro cgs) documented in the cuttings the observed magnetic gradient cannot be caused by a gradational horizontal change between the two major rock types observed in CGEH-1. These rock types are representative of the surface rocks in the area of the observed gradient. Assigning the metamorphic sequence with its average measured susceptibility (1118) to the zone at the high magnetic intensity end of the observed gradient and the granitic intrusives with their average susceptibility (547) to the low end will not give the computed change (3000) in susceptibility required to produce the observed gradient. Factors that could account for this apparent discrepancy are: 1) an increase in mafic content of the metamorphics within the high intensity zone giving an attendant increase in magnetic susceptibility, and 2) an attendant decrease in the

original or primary magnetite content of the granitic intrusives within the low intensity zone or the destruction of magnetite in the granitic intrusives as a result of hydrothermal alteration. Some combination of these factors is most likely. Measurements of the magnetic susceptibility of outcrop samples along the line of profile, Plate III, are required to determine to what degree each of these factors contribute to the observed gradient. If it can be shown that magnetite destruction is a significant factor, this would have an important bearing on the interpretation of the magnetic low outlined on Plate III.

Structure

Based on analyses of seismic activity, Weaver and Walter (1977) describe a northwest trend of right-lateral, strike-slip faulting, the Haiwee trend, and a complimentary northeast trend of left-lateral, strike-slip faulting, the Red Hill trend. These geographic names are given to the two structural zones shown on Plate III since their southwestern and northwestern portions conincide, respectively, to the Red Hill and the Haiwee trends described by Weaver and Walter. Plate III shows the Haiwee trend corresponds to a zone of low magnetic intensity and several similarly trending faults shown on Plate I. The Red Hill trend is well defined on the magnetic map from Sugarloaf Mountain to the southwest. The major east-northeast fault mapped by Hulen (1978), Plate III, is evidence for a continuation of this trend to the northeast through Devil's Kitchen and Coso Hot Springs. The trace of this fault is delineated by the canyon through the eastern side of the Coso Range between Devil's Kitchen and Coso Hot Springs. The fault is quite important since the fumerolic activity is either on or along the projection of its trace. The

deeply-incised, northeast-trending canyons through the basalt flows east of Coso Hot Springs may be fault-related and as such could represent a continuation of the Red Hill structural zone. The USGS aeromagnetic map and geologic map show east-northeast magnetic trends, topographic lineations and inferred faults that support the interpretation of a through-going, east-northeast structural zone. The structural zones shown on Plate III could help define zones of active tectonism by association with the zones of active seismicity.

Magnetic Low

The magnetic low outlined on Plate III is the most significant feature delineated by this survey with respect to the Coso geothermal system. It generally coincides with two other geophysical anomalies obviously related to the geothermal system, a bedrock electrical resistivity low (Fox, 1978) and an area of high, near-surface temperatures defined by LeSchack (1977). The highest measured rate of heat flow, 18 HFU (Combs, 1975), and evidence for hydrothermal bedrock alteration and magnetite destruction, mapped by Hulen (1978), both occur within its boundary. This direct evidence of magnetite destruction (although not pervasive), the lack of magnetic expression of the rhyolite dome at RP-15a, and the analysis of the magnetic field gradient (Figure 3), give reason to think that the magnetic low is partially due to magnetite destruction which is directly related to hydrothermal fluids within the geothermal system. The southern one-half of the low is due, in part, to an induced polarization low associated with the zone of high magnetic intensity at the southern boundary of the low. A polarization low is induced by the earth's magnetic field at the northern boundary of a magnetic source

with higher magnetic susceptiblility than its host rock.

Comparison of High- and Low-Altitude Magnetic Maps

Plate VI shows a portion of the USGS, 7000 foot (2135 m) constant-barometric-altitude, aeromagnetic map that corresponds with the low altitude survey. This map shows what can be considered to be an 'upward continuation' of the observed low-altitude magnetic field (Plate III). Local anomalies over volcanic domes and those resulting from terrain effects are completely attenuated while the west-northwest trending zones of contrasting magnetic intensity, Plate III, the two complimentary structural trends and the associated magnetic low are still readily apparent.

SUMMARY AND CONCLUSIONS

A low-altitude aeromagnetic survey of a portion of the Coso Hot Springs KGRA has defined a pronounced magnetic low that could help delineate the geothermal system. The magnetic low has an areal extent of approximately 10 sq mi (26 sq km). Direct and indirect evidence indicates that this anomaly is due, in part, to magnetite destruction by hydrothermal solutions associated with the geothermal system. It is significant that this anomaly generally coincides with two other geophysical anomalies which are directly associated with the system: 1) a bedrock electrical resistivity low, and 2) an area of relatively high near-surface temperatures.

The magnetic low occurs at the intersection of two major structural zones which are defined by magnetic lineations, mapped faults, and topographic features which coincide with a complementary set of strike-slip fault zones determined from seismic activity (Weaver and Walter, 1977). The intersection of these two zones of active tectonism probably served as the locus for emplacement of a pluton at depth, above which are observed the coincidental geophysical anomalies and surface manifestations related to the geothermal system.

ACKNOWLEDGEMENTS

This work was funded by Department of Energy, Division of Geothermal Energy contract EY-76-S-07-1601. Related Coso studies are being continued under Department of Energy, Division of Geothermal Energy contract EG-78-C-07-1701. The author thanks Charles R. Bacon and William F. Isherwood of the United States Geological Survey for their review of and comments on this report.

REFERENCES

Combs, J., 1975, Heat flow and microearthquake studies, Coso geothermal area, China Lake, California: Final Report, Contract No. NOO 123-74-2099, Program code 4F10, sponsored by ARPA.

Duffield, W. A., and Bacon, C. R., 1977, Preliminary geologic map of the Coso volcanic field and adjacent areas, Inyo County, California: US Geol. Sur. Open File Map 77-311, 2 sheets.

Fox, R. C., 1978, Dipole-dipole resistivity survey of a portion of the Coso Hot Springs KGRA, Inyo County, California: UURI-ESL Report, DOE Contract EY-76-S-07-1601.

Furgerson, R. B., 1975, Progress report on electrical resistivity studies Coso Geothermal Area, Inyo County, California: Naval Weapons Center Tech. Pub. S497., China Lake, Calif.

Hulen, J. B., 1978, Geology and alteration of the Coso Hot Springs Geothermal Area, Inyo County, California: UURI-ESL Report, DOE Contract EG-78-C-07-1701.

Lanphere, M. A. and Dalrymple, G. B., 1975, K-Ar ages of Pleistocene rhyolitic volcanism in the Coso Range, California: Geology, V. III, pp. 339-341.

LeSchack, L. A., Lewis, J. E., and Chang, D. C., 1977, Rapid reconnaissance of geothermal prospects using shallow temperature surveys: Semi-annual technical report (December). Development and Resources Transportation Co., DOE Contract EG-77-C-01-4021.

USGS, 1976, Residual Magnetic Intensity Map, Coso Hot Springs, California: Open File Report 76-698.

Weaver, C. S. and Walter, A. W., 1977, Strike-slip fault zones and crustal spreading in the Coso Range, California: USGS Preliminary Report (in preparation).

Geology after Duffield and Bacon, 1977

PLATE I

GEOLOGIC/TOPOGRAPHIC BASE MAP

COSO HOT SPRINGS, KGRA

INYO COUNTY, CALIFORNIA

BY EARTH SCIENCE LABORATORY

UNIVERSITY OF UTAH RESEARCH INSTITUTE

R 38 E

R 39 E

T 21 S

T 22 S

Flown: September, 1977
Survey by: Aerial Surveys, SLC, Utah
Flight Altitude: 750 feet above mean terrain *
Flight Line Spacing: 1/4 mile
Flight Line Direction: N-S
Total Magnetic Field Intensity: - 51,500 gammas
Inclination, Magnetic Field: -61°
Declination, Magnetic Field: - 16°

* Maintained by digital readout from radar altimeter and analog recorded.

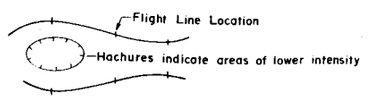

Topographic base maps for area:
USGS 15 minute topographic series-
Haiwee Reservoir, Coso Peak, Little Lake and Mountain Springs Canyon quads.

Contoured values are total magnetic field value minus 50,000 gammas.

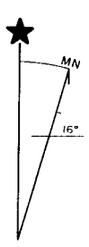

PLATE II

TOTAL FIELD AEROMAGNETIC MAP

COSO HOT SPRINGS, KGRA
INYO COUNTY, CALIFORNIA

BY EARTH SCIENCE LABORATORY
UNIVERSITY OF UTAH RESEARCH INSTITUTE

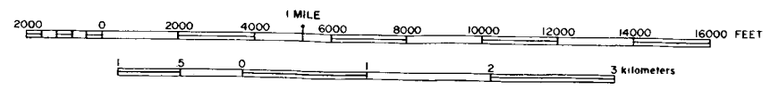

R 38 E

R 39 E

T 21 S

T 22 S

HIGH MAGNETIC INTENSITY

INTERMEDIATE MAGNETIC INTENSITY

LOW MAGNETIC INTENSITY

HIGH MAGNETIC INTENSITY

INTERMEDIATE MAGNETIC INTENSITY

LOW MAGNETIC INTENSITY

BOUNDARIES OF HAIWEE TREND

SOUTHERN BOUNDARY OF HAIWEE

STRUCTURAL ZONE

NORTHERN BOUNDARY OF WILSON CANYON FAULT SYSTEM

RED HILL TREND

RED HILL TREND

RP-1

RP-2

RP-3

RP-4

RP-5

RP-6

RP-7

RP-8

RP-9

RP-10

RP-11

RP-12

RP-13

RP-14

RP-15

RP-15a

RP-16

RP-17

RP-18

RP-19

RP-20

RP-21

RP-22

RP-23

RP-24

RP-25

RP-26

RP-27

RP-28

RP-29

RP-30

RP-31

RP-32

RP-33

RP-34

RP-35

RP-36

RP-37

RP-38

RP-39

RP-40

CGEH-1

location of profile shown on Figure 3

COSO HOT SPRINGS

DEVILS KITCHEN

RED HILL TREND

BOUNDARIES OF HAIWEE TREND

RP-11 Magnetic Source

Magnetic low; coincident with thermal and resistivity anomalies and alteration and geothermal indicators

Zones of contrasting magnetic intensity

Major magnetic trend

Inferred fault based upon topographic expression

Fault mapped by Hulen (1978) and projected westward on basis of resistivity data

MN

16°

PLATE III

INTERPRETIVE OVERLAY
COSO HOT SPRINGS, KGRA
INYO COUNTY, CALIFORNIA

BY EARTH SCIENCE LABORATORY
UNIVERSITY OF UTAH RESEARCH INSTITUTE

1 MILE
2000 0 2000 4000 6000 8000 10000 12000 14000 16000 FEET

1 .5 0 1 2 3 kilometers

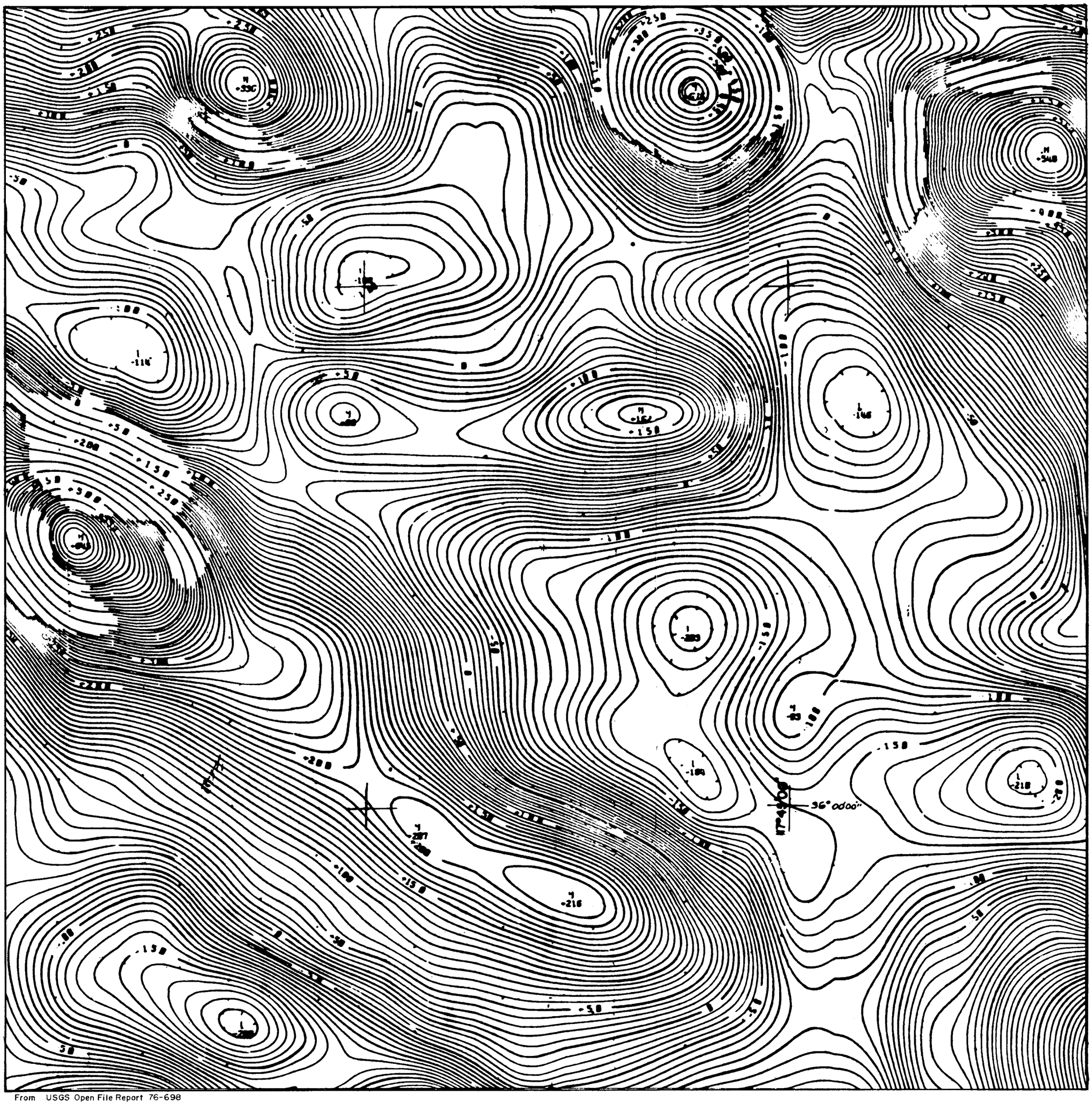

From USGS Open File Report 76-698

Portion of USGS RESIDUAL MAGNETIC INTENSITY MAP, COSO HOT SPRINGS, INYO COUNTY, CALIFORNIA

1 .5 0 1 2 3

Scale in kilometers

PLATE IV

EXPLANATION TO ACCOMPANY PRELIMINARY GEOLOGIC MAP OF THE COSO VOLCANIC FIELD AND ADJACENT AREAS, INYO COUNTY, CALIF.

BY WENDELL A. DUFFIELD AND CHARLES R. BACON

1977

CORRELATION OF MAP UNITS

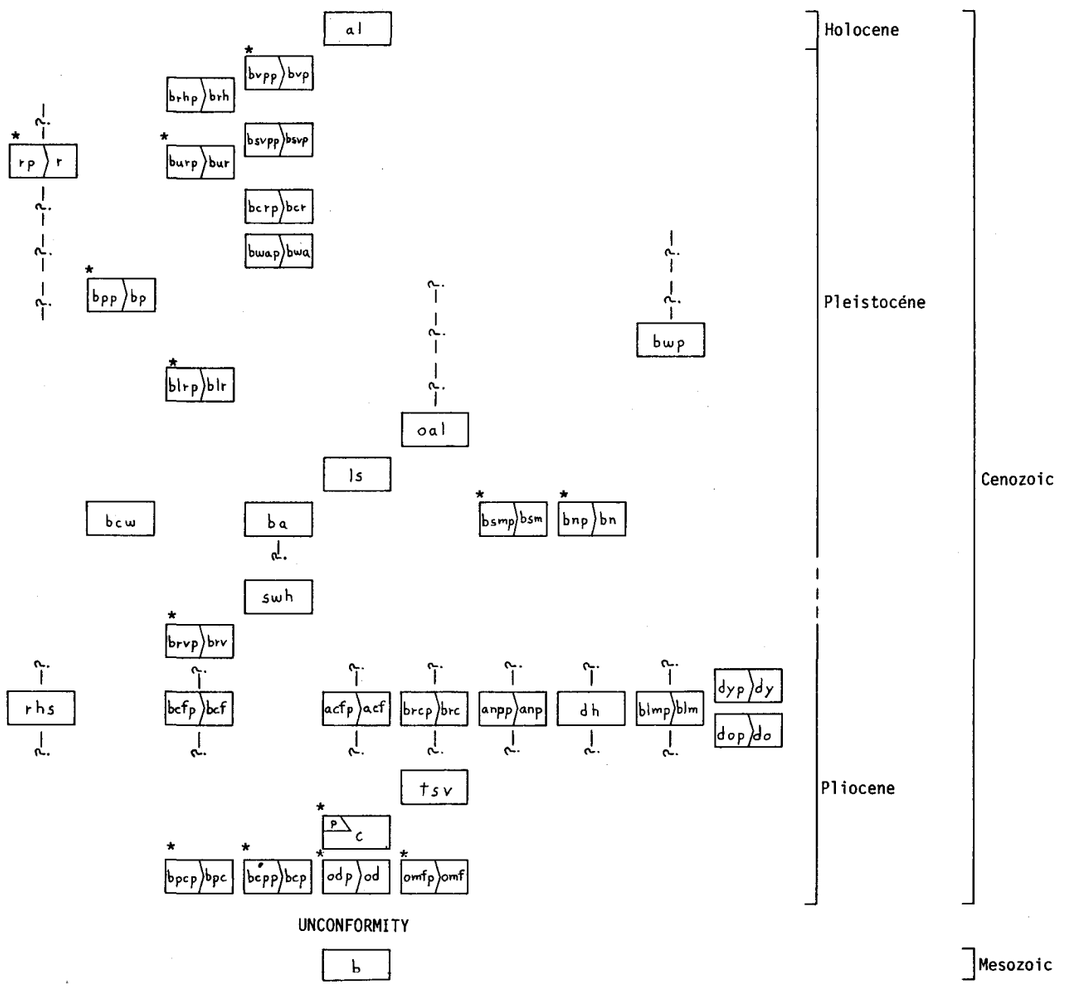

Note: The relative ages of units in the vertical columns are well established, whereas some of the implied relative ages for units of different columns are not well established. See descriptions of map units for known stratigraphic relations, and table for K/Ar ages. Asterisk denotes unit with K/Ar age.

DESCRIPTION OF MAP UNITS

al — ALLUVIUM Includes coarse alluvial fan deposits, stream deposits of gravel, sand and silt, wind blown sand, and deposits of silt and clay in closed depressions.

oal — OLD ALLUVIUM Includes predominantly sand to boulder-rich alluvial fan and fluvial deposits; probably ranges in age from late or middle Pleistocene to Holocene; distinguished from unit al by being partly dissected; oldest(?) part of this unit overlain by unit blr south-southeast of Little Lake.

rp / r — RHYOLITE OF THE COSO GEOTHERMAL FIELD Thirty-seven separate extrusions of sparsely porphyritic, homogeneous rhyolite (r) and associated pyroclastic deposits (rp); rp includes minor playa deposits in closed depressions; rhyolite forms steep-sided, 40 to 350 meter-high domes, several of which are overlapping and three of which developed flows about 1 km long; flows and domes are covered by blocky pumiceous to perlitic carapaces through which ribs and spines of obsidian protrude locally; rhyolite contains no more than 2 percent and generally less than 1 percent phenocrysts, all less than 1 mm long; some or all of the phases quartz, sanidine, oligoclase, Fe-Ti oxides, biotite, hornblende, clinopyroxene, orthopyroxene and fayalite are present in each dome; pyroclastic deposits of pumice and obsidian together with fragments of Mesozoic basement rocks form explosion rings around some domes and a mantle over the entire area of the dome field; some domes carry scattered basaltic xenoliths and rare fragments of Mesozoic basement rocks; Pleistocene domes and basalt flows overlap in space and time; Pleistocene basalt units bp, bsm, and bcw are overlain by rhyolite pyroclastics from adjacent domes; field relations in the vicinity of Volcano Peak indicate the following succession: (1) eruption of basalt of Rose Valley (brvp) or eruption of a rhyolite dome (no overlapping relations), (2) eruption of basalt of Upper Little Lake Ranch (bur), (3) eruption of a rhyolite dome, (4) eruption of basalt of Volcano Peak (bvp); K/Ar ages of domes range from 0.96 ± 0.19 to 0.041 ± 0.021 m.y. (Lanphere and others, 1975).

bvpp / bvp — BASALT OF VOLCANO PEAK Flows (bvp), cinder-bomb cone (bvpp), and adjacent cinder mantle (bvpp) of porphyritic, vesicular basalt; contains 1 percent of 0.2-1 mm olivine, 3 percent 0.2-1 mm yellowish clinopyroxene with rare opaque inclusions, 15 percent 0.5-4 mm plagioclase, and rare 0.6-3 mm embayed quartz in a granular groundmass of olivine, clinopyroxene, opaques, and plagioclase; olivine, clinopyroxene, and plagioclase phenocrysts commonly intergrown in clots; overlies units bsvp, bcr, r, bur, bwp and brv; aa flow surface and flow channels are well preserved; flows followed stream valleys; K/Ar age 0.038 ± 0.032 m.y. (Lanphere and others, 1975); probably the youngest volcanic unit in the map area; estimated average thickness of flows 2-6 meters.

bsvpp / bsvp — BASALT SOUTH OF VOLCANO PEAK Flow (bsvp), cinder-bomb cone (bsvpp) and adjacent cinder mantle (bsvpp) of porphyritic, vesicular basalt; flow was fed from vent marked by the cone 0.8 km south of Volcano Peak; contains 3 percent of 0.1-0.6 mm olivine, 2 percent of 0.1-1 mm clinopyroxene commonly in clots and containing rare opaque inclusions, and 15 percent of 0.2-4 mm plagioclase with olivine inclusions in an aphanitic groundmass; overlies unit bcr; and is overlain by unit bvp; aa flow surface and flow channels well preserved; estimated thickness of flow 2-6 meters.

DEPARTMENT OF THE INTERIOR
UNITED STATES GEOLOGICAL SURVEY

U.S. GEOLOGICAL SURVEY
OPEN FILE MAP
77-311
SHEET 2 OF 2

bcrp / bcr — BASALT OF CINDER RIDGE Seven cinder-bomb cones (bcrp) adjacent cinder mantle (bcrp), and at least two flows (bcr) of porphyritic, vesicular basalt; youngest flow contains about 2 percent of 0.2 mm and smaller olivine, 2 percent of 0.1-0.8 mm pale yellow clinopyroxene, 10 percent of 0.1-1 mm plagioclase, and 3 percent of 1-10 mm plagioclase in an aphanitic groundmass; youngest flow contains relatively more plagioclase and less olivine phenocrysts than underlying flow; overlies units bwa, swh, blr, and ba, and is overlain by units bvp, and bsvp; much or all of youngest flow appears to have issued from most southerly of five aligned cinder cones; aa flow surface and flow channels well preserved; magnetic polarity normal; total thickness about 3-8 meters.

bwp — BASALT SOUTHWEST OF VOLCANO PEAK Partly buried basalt cinder cone; overlain by unit bvp.

bwap / bwa — BASALT WEST OF AIRPORT LAKE Flow (bwa), cinder cone (bwap), and adjacent cinder mantle (bwap) of porphyritic, vesicular basalt; contains 1 percent of 0.1-0.2 mm opaque mineral (titanomagnetite?), 2 percent of 0.1-0.8 mm olivine, and 7 percent of 0.3-2 mm plagioclase in a groundmass of felted plagioclase laths, granular olivine, pyroxene, and opaque mineral; overlies units swh, ba, and is overlain by unit bcr; strand lines eroded into this unit along southwest edge of Airport Lake; aa surface and flow channels preserved; magnetic polarity normal; 2 to 4 meters thick.

bpp / bp — BASALT OF MERCURY PROSPECT Flow (bp) and cinder cone (bpp) of vesicular basalt; contains 1 percent 0.1-0.3 mm olivine, 0.5 percent 0.1-0.6 mm opaques, and 8 percent 0.2-1.5 mm plagioclase in a groundmass of granular olivine, opaques, pyroxene, and plagioclase laths; xenoliths of Mesozoic granitic basement rocks common; overlies units bcw, c, omf, od, and oal; flow channel and aa surface preserved locally; flow followed a stream channel into Airport Lake; about 2 to 7 meters thick; magnetic polarity normal; K/Ar age 0.234 ± 0.022 m.y.

brhp / brh — BASALT OF RED HILL Flow (brh) and cinder-bomb cone (brhp) and adjacent cinder blanket (brhp) of porphyritic, vesicular basalt; contains 1 percent 0.1-1 mm olivine with opaque inclusions, less than 1 percent yellowish clinopyroxene, 2 percent 0.1-1 mm plagioclase, and 5 percent 1-3 mm plagioclase in groundmass of felted plagioclase laths granular olivine, opaques, and pyroxene; xenoliths of Mesozoic granitic basement rocks common; overlies units bur and blr; flow followed Pleistocene Owens River channel at least 16 km downstream into Indian Wells Valley; aa to pahoehoe flow surface well preserved locally; magnetic polarity normal; about 4 to 10 meters thick.

burp / bur — BASALT OF UPPER LITTLE LAKE RANCH Flow (bur) and cinder cone (burp) of vesicular basalt; contains 1 percent 0.2-1 mm olivine and 2 percent 0.3-1 mm plagioclase in a coarse grained, sub-ophitic groundmass of olivine, opaques, lavender clinopyroxene, and plagioclase laths; overlies units blr and brv, and is overlain by units bvp and brh; flowed down Pleistocene Owens River channel for at least 15 km; pahoehoe to aa flow surface preserved locally; magnetic polarity normal; thickness ranges from about 5 meters to a maximum exposed thickness of 25 meters where lava ponded in Owens River channel near Little Lake; overlain by rhyolite pyroclastics of unit r with K/Ar age of 0.077 ± 0.008 m.y. (see Lanphere and others, 1975, sample no. 1); K/Ar age 0.140 ± 0.089.

blrp / blr — BASALT OF LOWER LITTLE LAKE RANCH Cinder-bomb cone (blrp) and at least two flows (blr), of porphyritic vesicular basalt; contains 1 percent 0.1-0.4 mm opaques (titanomagnetite?), less than 1 percent olivine, 2 percent 0.2-1 mm pale yellow clinopyroxene with opaque inclusions up to 0.1 mm, and 7 percent 0.2-3 mm plagioclase with common sieved cores in groundmass of granular olivine, opaques, clinopyroxene, and felted plagioclase laths; xenoliths of Mesozoic basement rocks present; overlain by units bcr, brh, and bur, and overlies unit oal; total thickness 3-10 meters magnetic polarity normal; K/Ar age of upper flow 0.399 ± 0.045 m.y. and K/Ar age of lower flow 0.486 ± 0.108 m.y.

ls — LANDSLIDE Landslide debris of Sierra Nevada escarpment near Little Lake; appears to be overlain by unit oal.

bcw — BASALT OF COSO WASH At least three flows of porphyritic, vesicular basalt; contains 3 percent 0.1-1 mm olivine with opaque inclusions, 1 percent 1-4 mm olivine, less than 1 percent 0.1-0.2 mm opaques, 2 percent 0.2-0.5 mm brownish clinopyroxene, rare clinopyroxene up to 2 mm, and 20 percent 0.3-2 mm plagioclase with opaque inclusions in a fine-grained groundmass of granular olivine, opaques, pyroxene, and plagioclase; smaller phenocrysts commonly intergrown in clots; xenoliths of Mesozoic basement rocks common; overlain by unit bp; flow followed stream channel; vent area is probably buried by rhyolite dome at the upstream end of the flow; magnetic polarity normal; aa surface preserved locally; thickness ranges from 7 to at least 25 meters.

ba — BASALT OF AIRPORT LAKE Porphyritic vesicular basalt flows; contain about 3 percent 0.05-6 mm olivine, 1 percent 0.2-1.5 mm clinopyroxene, 5 percent 0.1-1 mm plagioclase, 5 percent 0.5-6 mm plagioclase with sieved cores, and less than 1 percent 0.5-3 mm quartz in a groundmass of granular olivine, opaques, pyroxene, and plagioclase laths; phenocrysts commonly in clots; overlies unit swh and is overlain by units bcr and bwa; columnar jointing present locally; thickness about 3 to 7 meters.

bsmp / bsm — BASALT OF SUGARLOAF MOUNTAIN Flow (bsm) and associated cinder deposits (bsmp) of porphyritic, vesicular basalt; contains about 10 percent 0.1-4 mm olivine, less than 1 percent 0.4-6 mm clinopyroxene, 20 percent 0.2-1 mm plagioclase, and 3 percent 1-10 mm plagioclase in a fine-grained groundmass of plagioclase laths and granular olivine, clinopyroxene, and opaques; flow followed stream channel; about 3-5 meters thick; K/Ar age 1.08 ± 0.06 m.y.

bnp / bn — BASALT OF NAMELESS HILL Two flows (bn) and two cinder-bomb deposits (bnp) of microporphyritic, vesicular basalt. Contains 2 percent 0.3 mm and smaller olivine and 7 percent 0.2-2 mm plagioclase in a groundmass of granular olivine, opaques, pyroxene, and plagioclase; flows followed stream valleys; xenoliths of Mesozoic basement rocks common; estimated thickness 3-6 meters, K/Ar age 1.07 ± 0.12 m.y.

swh — SEDIMENTARY ROCKS OF THE WHITE HILLS Includes interbedded conglomerate, sandstone, siltstone, silty claystone, and tufa; apparently grades laterally into cobble to boulder fanglomerate near the southwest corner of Airport Lake; overlain by units ba, bwa, blr, and bcr; some beds contain reworked, rounded pumice lapilli of unit p, indicating that unit swh is younger than the Coso Formation; contrasting mammalian fauna indicate this same age relation (Roland von Huene, oral commun., 1976).

brvp / brv — BASALT OF ROSE VALLEY Four cinder-bomb cones (brvp) and three flows (brv) of porphyritic, vesicular basalt; contains 2-8 percent 0.1-2 mm olivine, 2-6 percent 0.2-2 mm yellowish clinpyroxene, and 8-15 percent 0.2-4 mm plagioclase in a fine-grained groundmass of plagioclase and granular olivine, opaques, and pyroxenes; olivine and/or clinopyroxene phenocrysts commonly contain opaque inclusions up to 0.2 mm; phenocrysts commonly broken or rounded and embayed; glomero-porphyritic clots, xenoliths of Mesozoic basement rocks, and rounded quartz grains up to 0.5 mm present locally; overlain by units bur and bvp; maximum exposed thickness of flows 2-4 meters; K/Ar age 2.06 ± 0.34 m.y.

rhs — RHYOLITE SOUTH OF HAIWEE SPRING Dome or plug of flow banded, porphyritic rhyolite; contains about 1 percent 0.5-2 mm quartz, 1 percent 0.3-1 mm plagioclase, rare 1 mm sanidine, and rare 0.2-0.5 mm brown biotite in a matrix of gray devitrified rock or green hydrated, perlitic glass; bounded by normal fault on east; exposed thickness about 50 meters.

bcfp / bcf — BASALT OF UPPER CENTENNIAL FLAT Two cinder deposits (bcfp) and several basalt flows (bcf) averaging a few meters thick; contains about 1 percent or less of ≤1 mm olivine; overlies Coso Formation, unit c, just north of map area (see Hall and MacKevett, 1962).

blmp / blm — BASALT OF SILVER MOUNTAIN Two cinder deposits (blmp) and several vesicular, porphyritic lava flows (blm) averaging a few meters thick; contains 0.5-1.0 percent 0.5-2.0 mm olivine and 0.5-1.0 percent 0.5-2.0 mm plagioclase, with rare crystals of each as large as 5 mm in an intergranular groundmass of clinopyroxene, olivine, and plagioclase; contemporaneous with unit acf; maximum thickness about 30 meters.

acfp / acf — ANDESITE OF CACTUS FLAT Interlayered cinders and flows (acfp) and flows (acf) averaging 10 or more meters thick of porphyritic andesite; contains about 5 percent 1-4 mm plagioclase, 1 percent 0.5-2 mm pleochroic orthopyroxene, 1 percent 0.3-0.5 mm clinopyroxene, and less than 1 percent 0.3-0.5 mm olivine, in an intergranular groundmass of pyroxene and plagioclase; erupted from lava-cinder shield at north end of Cactus Flat; overlies Coso Formation (unit c) and is contemporaneous with unit blm.

brcp / brc — BASALT OF RENEGADE CANYON Five cinder cones ($brcp_{1-5}$), three eroded cinder deposits ($brcp_{6-8}$), and associated lava flows (brc, $brc_{1-4,8}$) averaging a few meters thick; flows near some cones can be traced to source vents on bases of morphology and phenocryst assemblages; phenocrysts include 3-10 percent 0.5-3.0 mm plagioclase, 1-5 percent 0.1-2.0 mm olivine and 1-4 percent 0.2-1.5 mm clinopyroxene; subunits brc_1, brc_3, and locally brc contain 1 percent 1-3 mm rounded grains of quartz; part of subunit brc_8 contains only plagioclase and olivine phenocrysts; maximum exposed thickness about 170 meters; overlies units od, omf, tsv, and p.

anpp / anp — ANDESITE NORTHWEST OF PETROGLYPH CANYON Flow (anp) and associated pyroclastic deposit (anpp) of porphyritic basaltic andesite; near vent area contains about 2 percent 0.1-0.6 mm olivine, 2 percent 0.3-0.8 mm clinopyroxene, 10 percent 0.2-4.0 mm plagioclase, and rare 1-1.5 mm rounded quartz in a fine-grained matrix of clinopyroxene, opaques, and plagioclase; thickness ranges from about 5-30 meters; phenocryst content and thickness decrease away from vent area; overlies units c, p, bpc, and omf; magnetic polarity normal.

dh — DACITE OF HAIWEE RIDGE Flows of porphyritic dacite; contains rare 0.02 mm zircon, rare 0.1 mm apatite, rare 0.1-0.7 mm orthopyroxene with amphibole rims on larger crystals, rare 0.1 mm clinopyroxene(?), 1 percent 1-2 mm quartz, 1 percent 0.05-0.2 mm opaques, 3 percent 0.2-1.5 mm brown biotite with opaque and feldspar inclusions, 3 percent 0.2-1.7 mm greenish brown amphibole with opaque, feldspar, and biotite inclusions, and 15 percent 0.1-6.0 mm plagioclase with inclusions of most other phenocryst phases in a glassy groundmass now largely composed of feldspar and other microlites; overlies unit c; highly flow banded; columnar jointing developed where ponded; average thickness about 25 meters; ponded to at least 200 meters south of Haiwee Reservoir; Evernden and others (1964) report K/Ar age of 2.1 m.y.

ANALYTICAL DATA AND CALCULATED POTASSIUM-ARGON AGES FOR VOLCANIC ROCKS OF THE COSO VOLCANIC FIELD††

BY G. BRENT DALRYMPLE

Location	Map unit	Sample number	Material	K_2O† wt. %	Argon: Weight (gms)	Argon: $^{40}Ar_{rad}$ (10^{-12} mol/gm)	Argon: $\frac{100\ ^{40}Ar_{rad}}{^{40}Ar_{total}}$	Calculated Age* (10^6 years)
NE1/4sec6 T23S,R38E	bur	75G301	basalt	1.356 ± 0.004(4)	18.325 20.134	0.222 0.312	1.0 1.6	0.140 ± 0.089
SW1/4sec35 T22S,R39E	bp	75G314	basalt	1.525 ± 0.007(4)	15.169 25.247	0.529 0.505	7.7 7.6	0.234 ± 0.022
NE1/4sec32 (upper flow) T23S,R38E	blr	75G305	basalt	1.789 ± 0.010(4)	19.561	1.029	8.6	0.399 ± 0.045
NE1/4sec32 (lower flow) T23S,R38E	blr	75G306	basalt	1.610 ± 0 003(4)	18.995	1.126	5.0	0.486 ± 0.108
NW1/4sec26 T23S,R38E	bn	75G308	basalt	1.312 ± 0.004(4)	20.230 21.858	1.638 2.118	3.8 9.9	1.07 ± 0.12
SE1/4sec14 T22S,R38E	bsm	75G309	basalt	1.530 ± 0.009(4)	29.248 29.693	2.317 2.395	11.4 21.2	1.08 ± 0.06
SE1/4sec21 T22S,R38E	brv	75G304	basalt	1.738 ± 0.005(4)	14.052 14.912	6.29 4.84	4.1 5.6	2.06 ± 0.34
NE1/4sec13 T20S,R37E	c	9-85-2	sanidine	12.315(2)	3.835	54.88	66.2	3.09 ± 0.09
NE1/4sec23 T21S,R38E	p	9-8-11	biotite plagioclase	6.475(2) 0.458(2)	1.151 5.863	22.975 2.004	2.4 16.0	2.46 ± 0.98 3.03 ± 0.20
NW1/4sec11 T22S,R39E	p	13-113-6	plagioclase	0.518(2)	6.108	2.203	24.4	2.95 ± 0.13
SW1/4sec15 T22S,R39E	od	75G315	biotite plagioclase	8.24(2) 0.696(2)	1.813 7.848	40.58 2.210	43.1 3.1	3.42 ± 0.10 2.20 ± 0.70
NE1/4sec28 T20S,R39E	bcp	8-193-2	basalt	1.786 ± 0.004(4)	21.163 19.000	9.218 9.312	28.0 47.1	3.60 ± 0.08
NW1/4sec13 T22S,R39E	omf	13-113-15	basalt	1.042 ± 0.005(4)	16.000 16.000	4.686 4.569	6.7 7.9	3.10 ± 0.22
SW1/4sec3 T21S,R39E	omf	8-195-2	basalt	1.713 ± 0.007(4)	20.110 19.990	8.700 8.794	25.5 42.3	3.54 ± 0.08
NE1/4sec15 T22S,R39E	omf	8-199-6	basalt	0.857 ± 0.004(4)	20.458 15.225	4.188 5.202	15.8 8.2	3.67 ± 0.16
NE1/4sec5 T22S,R40E	bpc	13-113-17	basalt	0.726 ± 0.002(4)	19.530 17.627	3.076 3.169	16.3 16.4	2.98 ± 0.12
SE1/4sec12 T21S,R39E	bpc	13-111-1	basalt	0.708 ± 0.004(4)	18.711	3.572	20.7	3.50 ± 0.19
SE1/4sec10 T21S,R39E	omf	8-196-2	basalt	1.318 ± 0.012(4)	19.991 19.688	6.941 6.925	37.1 33.7	3.66 ± 0.08

† Errors are calculated standard deviations. Number of analyses in parentheses.

* $\lambda_\beta = 4.963 \times 10^{-10}\ yr^{-1}$, $\lambda_\epsilon = 0.572 \times 10^{-10}\ yr^{-1}$, $\lambda'_\epsilon = 8.78 \times 10^{-13}\ yr^{-1}$, $^{40}K/K = 1.167 \times 10^{-4}$ mol/mol. Errors are estimated standard deviation of precision.

†† Potassium measured by lithium metaborate fusion and flame photometry. Argon measured by isotope dilution mass spectrometry.

dyp > dy — YOUNGER DACITE EAST OF COSO VALLEY Small cinder deposit (dyp) and thick flow (dy) of flow banded dacite; contains less than 1 percent 1.2-2 mm quartz, 10 percent 0.6-6 mm plagioclase, less than 1 percent 0.1-0.6 mm brown amphibole, now mostly replaced by iron oxide, less than 1 percent 0.3-1.5 mm orthopyroxene, rare 0.5-0.7 mm clinopyroxene, and rare 0.3 mm biotite in a groundmass of opaque, pyroxene, and feldspar microlites in devitrified glass; overlies units bpc, omf, c, and do; thickness 10 to at least 60 meters.

dop > do — OLDER DACITE EAST OF COSO VALLEY Cinder deposit (dop) and thick flow (do) of platy, flow banded dacite; contains 1 percent 0.6-1 mm quartz, 3 percent 0.6-3 mm plagioclase, less than 1 percent 0.3-1 mm brown amphibole, now mostly replaced by iron oxide, less than 1 percent 0.3-1.2 mm ragged brown biotite, less than 1 percent 0.2-0.8 mm clinpyroxene, commonly in clots, and 1 percent 0.2-5.0 mm orthopyroxene, commonly with cores of up to 1 mm forsteritic olivine in a groundmass of opaques, pyroxene, and feldspar microlites in devitrified glass; overlies units bcp and c and is overlain by unit dy; magnetic polarity normal; thickness 5 to at least 50 meters.

tsv — TUFF SOUTHWEST OF VOLCANO BUTTE Basaltic to andesitic pyroclastic deposit; well stratified vesicular ash and lapilli, with beds from a few to several centimeters thick, locally disturbed by volcanic bomb sags 0.3-1.0 meter in diameter; maximum exposed thickness about 6 meters; overlain by unit brc.

p > c — COSO FORMATION Includes fanglomerate of Mesozoic basement rocks, arkosic sandstone, tuffaceous sandstone and siltstone, tuffaceous lacustrine beds, and silicic tuff; fanglomerate, coarse-grained arkose, and tuff are predominant on the high slopes of Haiwee Ridge and interfinger with finer grained rocks and lacustrine beds to the north and west; north and east of Upper Cactus Flat and Coso Hot Springs, fanglomerate and interlayered hornblende-biotite pumice (p) predominate; overlies units b, od, bcp, bpc, and omf and is overlain by units acf, dh, bcf, do, dy, anp, and brc; K/Ar age of rhyolitic tuff in c is 3.09 ± 0.09 m.y.; K/Ar ages of p are 3.03 ± 0.20 m.y., 2.46 ± 0.98 and 2.95 ± 0.13 m.y.; Evernden and others (1964) report a K/Ar age of 2.3 m.y. for silicic tuff in c, inconsistent with results of present study.

omfp > omf — OTHER MAFIC LAVAS Flows from 2 to 20 meters thick (omf) and eroded cones (omfp) of porphyritic vesicular basalt to basaltic andesite; phenocrysts include up to 7 percent 0.1-2 mm olivine, 5 percent 0.2-1 mm greenish sector-zoned clinopyroxene, and 25 percent 0.2-3 mm oscillatory-zoned plagioclase in a fine grained groundmass of plagioclase laths, granular olivine, an opaque mineral, and clinopyroxene; glomeroporphyritic texture common; some flows contain 1 mm amphibole almost entirely replaced by opaque oxides; others contain plagioclase as large as 5 mm with sieved cores and clear rims, rare alkali feldspar as large as 3 mm, and rounded grains of quartz as large as 5 mm armored by a rind of clear, brown glass in turn rimmed with clinopyroxene; total phenocryst content generally less than 20 percent; some cinder deposits are in part dacitic; basalt dikes cut cinder cones locally; some flows west of Silver Peak superficially similar to those of unit bpc; overlies unit b, interfingers with units bpc and od, and is overlain by units bcp, c, p, brc, brc$_4$, bp, and oal; includes both normal and reversed magnetic polarities; K/Ar ages range from 3.10 ± 0.22 m.y. to 3.66 ± 0.08 m.y.

odp > od — OTHER DACITE Cinder deposits (odp) and flows and shallow intrusive bodies (od) predominantly of porphyritic biotite and/or hornblende dacite; includes minor porphyritic olivine or orthopyroxene andesitic flows near Volcano Butte; odp commonly includes mafic cinders admixed with dacitic cinders; dacite flows contain up to 30 percent 0.1-8 mm oscillatory-zoned plagioclase and various combinations of as much as 2 percent 0.8-4 mm rounded and embayed quartz, 5 percent 0.2-1.5 mm orthopyroxene, 3 percent 0.2-0.8 mm clinopyroxene, 15 percent 0.1-2.5 mm generally oxidized brown amphibole, 7 percent 0.1-1.5 mm brown biotite, 1 percent 0.2-0.5 mm opaque mineral, accessory 0.1-0.8 mm sphene and 0.1-0.2 mm zircon in a very fine-grained to glassy groundmass; as much as 1 percent 0.1-0.8 mm olivine present locally; rounded inclusions of andesite, basaltic andesite, and basalt a few millimeters to several meters in size account for as much as 30 percent of many outcrops; in such mixed rocks, coexistence of dacitic and more mafic liquids is indicated by interfingering and partial mixing on scale of a few millimeters; thickness ranges from roughly 20 meters to at least 300 meters; interfingers with units omf and bpc; overlain by units c, p, brc, tsv, bp, and oal; K/Ar ages 3.42 ± 0.10 and 2.20 ± 0.70 m.y.

bcpp > bcp — BASALT OF COSO PEAK Cinder deposits (bcpp) and a few flows (bcp) of porphyritic basalt; contains 0-5 percent 0.2-3 mm olivine with spinel inclusions and 1-3 percent 0.2-2 mm greenish sector-zoned clinopyroxene in a groundmass of granular opaques, olivine, clinopyroxene, and plagioclase laths; phenocrysts commonly occur in clots; locally contains granitic xenoliths and quartz grains; at least 10 meters thick; overlies units b and omf; overlain by unit p; magnetic polarity reversed; K/Ar age 3.60 ± 0.08 m.y.

bpcp > bpc — BASALT OF UPPER PETROGLYPH CANYON Cinder deposits (bpcp) and thin flows (bpc) of vesicular basalt; contains 3-5 percent 0.2-3 mm olivine with opaque inclusions and 5-10 percent 0.5-6mm oscillatory-zoned plagioclase in a coarse grained ophitic groundmass of bladed opaques, granular olivine, poikilitic brownish clinopyroxene, and plagioclase laths; typically displays vesicle cylinders and sheets, glomeroporphyritic clots, platy jointing near tops of flows, columnar jointing in flow interiors, and well-developed diktytaxitic texture; thickness 3 to at least 60 meters; overlies unit b, interfingers with units omf and od, and is overlain by units oal, c, p, anp, do, and dy; K/Ar ages 2.98 ± 0.12 and 3.50 ± 0.19 m.y.

b — UNDIFFERENTIATED BASEMENT ROCKS (Mesozoic) Principally granitic intrusive rocks of Mesozoic age; compositions range from granite to quartz diorite to quartz-free diorite or gabbro; textures range from medium- to coarse-grained to porphyritic with K-feldspar crystals up to 1.5 cm; mafic inclusions common, especially in south part of map area; metamorphic pendants as much as 0.5 km long present in east and northeast part of map area; generally northwest trending, Mesozoic(?) dikes of silicic and intermediate to mafic composition abundant locally.

EXPLANATION OF SYMBOLS

Contact, dashed where uncertain and dotted where concealed.

Fault, dashed where uncertain and dotted where concealed or inferred; bar and ball on down-thrown side. Dip of fault plane shown where known.

Topographic crest of ring of pyroclastic debris that partly surrounds some rhyolite domes.

Vents of mafic to intermediate lavas, represented by well preserved cinder cones, or eroded pyroclastic deposits. Dotted where concealed.

Strike and dip of stratified rocks, including mafic lava flows in east part of map area.

Attitude of steep flow foliation in unit dh.

Steeply dipping dike, in units omf and b only.

.140 ± .089 — K/Ar age in millions of years, with arrow to sample locality.

Direction of downslope ground slippage in landslide.

Note: In addition to being broken by the mapped faults, the Mesozoic basement rocks (b) that underlie that part of the field of rhyolite domes (r) south of Cactus Peak are shattered to pieces generally less than one meter in diameter and are locally hydrothermally altered, especially immediately west of Coso Basin and south and west of Coso Hot Springs.

REFERENCES

Evernden, J. F., Savage, D. E., Curtis, G. H., and James, G. T., 1964, Potassium-argon dates and the Cenozoic mammalian chronology of North America: Am. Jour. Sci., v. 262, p. 145-198.

Lanphere, M. A., Dalrymple, G. B., and Smith, R. L., 1975, K-Ar ages of Pleistocene rhyolitic volcanism in the Coso Mountains, California: Geology, v. 3, p. 339-341.

Hall, W. E., and MacKevett, E. M., Jr., 1962, Geology and ore deposits of the Darwin Quadrangle, Inyo County, California: U.S. Geol. Survey Prof. Paper 368, 87 p.

This map is preliminary and has not been reviewed for conformity with U.S. Geological Survey standards and nomenclature.